Assembly of Human Frataxin Is a Mechanism for Detoxifying Redox-Active Iron†

Heather A. O'Neill,‡ Oleksandr Gakh,‡ Sungjo Park,‡ Jin Cui,‡ Steven M. Mooney,‡ Matthew Sampson,§ Gloria C. Ferreira,§ and Grazia Isaya*,‡

Departments of Pediatric and Adolescent Medicine and of Biochemistry and Molecular Biology, Mayo Clinic College of Medicine, Rochester, Minnesota 55905, and Department of Biochemistry and Molecular Biology, College of Medicine, and H. Lee Moffitt Cancer Center and Research Institute, University of South Florida, Tampa, Florida 33612

Received July 19, 2004; Revised Manuscript Received September 8, 2004

ABSTRACT: Mitochondrial function depends on a continuous supply of iron to the iron−sulfur cluster (ISC) and heme biosynthetic pathways as well as on the ability to prevent iron-catalyzed oxidative damage. The mitochondrial protein frataxin plays a key role in these processes by a novel mechanism that remains to be fully elucidated. Recombinant yeast and human frataxin are able to self-associate in large molecular assemblies that bind and store iron as a ferrihydrite mineral. Moreover, either single monomers or polymers of human frataxin have been shown to serve as donors of Fe(II) to ISC scaffold proteins, oxidatively inactivated $[3Fe\text{-}4S]^+$ aconitase, and ferrochelatase. These results suggest that frataxin can use different molecular forms to accomplish its functions. Here, stable monomeric and assembled forms of human frataxin purified from *Escherichia coli* have provided a tool for testing this hypothesis at the biochemical level. We show that human frataxin can enhance the availability of Fe(II) in monomeric or assembled form. However, the monomer is unable to prevent iron-catalyzed radical reactions and the formation of insoluble ferric iron oxides. In contrast, the assembled protein has ferroxidase activity and detoxifies redox-active iron by sequestering it in a protein-protected compartment.

Mitochondria require mechanisms for ensuring a constant supply of reduced iron to the heme and iron−sulfur cluster (ISC)[1] biosynthetic pathways while limiting its potential toxicity. Mitochondrial iron mishandling is implicated in Friedreich ataxia (FRDA), a degenerative disease which results from an insufficient production of frataxin, a conserved nucleus-encoded mitochondrial protein (*1*). The function of frataxin has been the subject of intense study since the FRDA gene was identified (*1*). Seminal observations were made in yeast, where disruption of the frataxin gene was found to cause a loss of respiratory function, accumulation of large amounts of iron in mitochondria, mitochondrial DNA depletion, and increased sensitivity to exogenous H_2O_2 (*2*−*4*). In a short period of time, a large body of work in yeast, mouse, and cellular models of FRDA as well as FRDA patients collectively showed that frataxin is required for mitochondrial iron homeostasis, maintenance of ISC- and heme-containing enzymes, OXPHOS function, and protection from oxidative stress (*5*). We investigated the mechanism of frataxin and were the first to report that frataxin binds iron (*6*, *7*), a finding that has since been confirmed by other investigators (*8*−*11*). Currently, the predominant view is that frataxin is an Fe(II) chaperone. This is based upon *in vivo* studies showing that frataxin promotes the biosynthesis of ISC (*12*−*14*) and heme-containing proteins (*15*), and *in vitro* studies showing that frataxin can deliver Fe(II) to the ISC scaffold protein IscU in the first step of ISC synthesis (*9*), to ferrochelatase in the last step of heme synthesis (*10*, *16*), and to mitochondrial aconitase, converting the inactive $[3Fe\text{-}4S]^+$ enzyme to the active $[4Fe\text{-}4S]^{2+}$ form (*17*). The iron accumulation and oxidative damage associated with the loss of frataxin are considered secondary effects due primarily to impaired ISC synthesis (*14*). However, several lines of evidence suggest that frataxin also plays a direct role in the detoxification of redox-active iron. Increased levels of uncomplexed iron have been observed in mitochondria from FRDA cells (*18*), and a higher sensitivity to oxidative stress is a consistent feature of these cells, even when deficits of ISC-containing enzymes cannot be detected (*19*, *20*). Oxidative damage to mitochondrial DNA and proteins is the earliest detectable effect caused by reduced levels of frataxin in yeast (*21*), and similarly, lipoperoxides and oxidized proteins are an early finding in frataxin-deficient mice (*14*). Additional support for a direct role of frataxin in iron detoxification comes from a recent report that expression of human mitochondrial ferritin prevents the respiratory deficits, mitochondrial iron accumulation, and oxidative damage associated with the loss of frataxin in yeast (*22*). Together, these data suggest that increased oxidative stress is not a secondary effect but rather one of the primary consequences of frataxin deficiency, resulting from higher levels of labile redox-active iron no longer detoxified by frataxin.

An open question is how frataxin may serve as a donor of Fe(II) to diverse partner proteins and at the same time detoxify labile iron. We have shown that yeast frataxin acts

† This work was supported by NRSA 44748 from the NIH/NINDS (to H.A.O.), Grant RSG-96-05106-TBE from the American Cancer Society (to G.C.F.), a grant from the Muscular Dystrophy Association, and Grant AG15709 from the NIH/NIA (to G.I.).

* To whom correspondence should be addressed: Mayo Clinic College of Medicine, 200 First St. SW, Stabile 7-52, Rochester, MN 55905. Telephone: (507) 266-0110. Fax: (507) 266-9315. E-mail: isaya@mayo.edu.

‡ Mayo Clinic College of Medicine.

§ University of South Florida.

[1] Abbreviations: ISC, iron−sulfur cluster; FRDA, Friedreich ataxia; m-fxn, recombinant mature form of human frataxin residues 56−210; d-fxn, recombinant form of truncated human frataxin residues 78−210; BIPY, α,α′-bipyridine; CD, circular dichroism spectroscopy.

10.1021/bi048459j CCC: $30.25
Published on Web 12/18/2004

as both an Fe(II) chaperone and an Fe(III) storage molecule, and accomplishes these functions by assembling with itself (*16*). In addition, both monomeric and assembled forms of human frataxin have been shown to serve as Fe(II) donors *in vitro* (*9*, *10*, *17*), and to be present in human heart mitochondria (*37*). This evidence suggests that frataxin may use different molecular forms to achieve its diverse roles. To test this hypothesis, we have analyzed the properties of monomeric and assembled forms of human frataxin. This protein is normally encoded in the nucleus and translated in the cytoplasm as a 210-amino acid precursor polypeptide with a 55-amino acid mitochondrial-targeting sequence (*23*). The mature protein (residues 56−210) assembles into regular homopolymers during expression in *Escherichia coli* (*7*). However, the purified m-fxn monomer is stable and, unlike the yeast frataxin monomer (*6*), does not self-associate when incubated with iron *in vitro* (*7*, *8*). These features have enabled us to compare for the first time how monomeric frataxin and assembled frataxin handle redox-active iron.

MATERIALS AND METHODS

Reagents, Solutions, Biochemical Assays, and Expression Constructs. The source of all reagents, and the procedures for preparing buffers and stock solutions of Fe(II) and measuring the availability of Fe(II) to α,α′-bipyridine (BIPY) or ferrochelatase, and electrode oximetry were as described previously (*16*).

Recombinant Protein Expression and Purification. Monomeric and assembled m-fxn were expressed in *E. coli* and purified as described previously (*7*). Modifications that enable separation of the m-fxn monomer (residues 56−210) from its main degradation product (d-fxn, residues 78−210) are described in the Supporting Information. As analyzed by SDS−PAGE and protein staining, the purification procedure was reproducible with regard to protein yield and purity (>95% purity for m-fxn and d-fxn monomer and >85% for assembled m-fxn; Figure S1A,B of the Supporting Information). The identity and accurate molecular mass of each frataxin species were determined by electrospray ionization mass spectrometry. Prior to this analysis, assembled m-fxn was diluted 1-fold with acetonitrile to denature the protein, which revealed a single species with a molecular mass of 17 255 Da, corresponding within experimental error to that of the unmodified m-fxn monomer as purified from *E. coli* (*7*). Residual contaminating proteins present in assembled m-fxn preparations were identified by peptide mass fingerprinting or liquid chromatography/tandem mass spectrometry (Figure S1A−D of the Supporting Information). Purified proteins were stored in 10 mM HEPES-KOH at pH 7.3 and 4 °C, and used within 1 week. Protein concentrations were determined from the absorbance and extinction coefficient (ϵ_{280} = 42 800, 24 400, and 38 700 M^{-1} cm^{-1} for the m-fxn monomer, the d-fxn monomer, and assembled m-fxn, respectively). The same purification method used for assembled m-fxn was also used to generate mock preparations of assembled m-fxn from *E. coli* cells transformed with the empty vector. Recombinant mouse ferrochelatase was produced and purified as described previously (*24*) with the following modifications. (1) Triton X-100 (1%) was substituted with 0.5% cholate. (2) Solubilized proteins from the lysed cells were subjected to ultracentrifugation at 100000*g* for 60 min. (3) Ferrochelatase was eluted from the blue-Sepharose CL-6B resin with a linear NaCl gradient (from 0.5 to 2.0 M) in 20 mM Tris-HCl (pH 8.0) containing 10% glycerol. The purified protein was concentrated to 10 mg/mL in 20 mM Tris-HCl (pH 8.0) containing 1 M NaCl and 10% glycerol. Bovine brain calmodulin and horse spleen apoferritin (Sigma) were buffer exchanged into 10 mM HEPES-KOH (pH 7.3). All purified protein concentrations were calculated per subunit.

Protein Disassembly. In some DNA protection experiments, a preparation of assembled frataxin was split into two 1 mg aliquots and treated with either 2% SDS or buffer alone for 30 min at 24 °C. Both samples were incubated with 50 μL of Calbiosorb resin (Calbiochem) for 15 min at 24 °C and centrifuged at 2000*g* for 3 min at 24 °C. The protein was then repurified through a new Sephacryl 300 column and eluted with 120 mL of 10 mM HEPES-KOH (pH 7.3) and 150 mM NaCl. The protein recovery was ∼60 and 50% for buffer- and SDS-treated m-fxn, respectively. Fractions corresponding to assembled or disassembled m-fxn were pooled, buffer exchanged into 10 mM HEPES-KOH (pH 7.3), and concentrated with an Ultrafree-0.5 cell (5 kDa cutoff). SDS−PAGE and silver staining confirmed that the protein composition of assembled m-fxn was essentially unchanged and that no detectable contaminants were present in the disassembled protein fractions. Proteins were analyzed by far-UV circular dichroism spectroscopy (CD) on an Aviv spectrometer (model 215) (Aviv Associates/Protein Solutions) in a 0.2 cm path length cell in the continuous mode.

DNA Protection Assay. Plasmid DNA was purified from *E. coli* strain DH-5α (Invitrogen) using a QiaPrep Spin Miniprep kit (Qiagen) and suspended in Milli-Q deionized water. The following reagents were added in order to each 10 μL reaction mixture: 10 mM HEPES-KOH (pH 7.3), 20−200 μM protein, 160 ng of plasmid DNA, and Fe(II) or an equal volume of buffer. Each set of reaction mixtures was incubated at 30 °C, diluted with 3 μL of sample buffer (18% glycerol, 0.15% Bromophenol Blue) on ice, and immediately loaded on a 1% agarose gel (*25*). Ethidium bromide-stained DNA bands were visualized with an imaging system and quantified with Kodak 1D Image Analysis Software. In each case, the percentage of residual supercoiled DNA was calculated relative to a reaction mixture containing an identical concentration of assembled m-fxn but no added Fe(II) (*25*).

Iron Sequestration. Each reaction (500 μL) was started by adding 30 μM Fe(II) to an Eppendorf tube containing 3 μM protein in 10 mM HEPES-KOH (pH 7.3). No more than two reactions were analyzed simultaneously. After incubation for 10 or 60 min at 30 °C, each reaction mixture was cooled to 4 °C on ice, transferred to an ultrafiltration device (Ultrafree-0.5 cell, Millipore) with a molecular mass cutoff of 5 kDa, and centrifuged at 20800*g* for 8 min at 4 °C. The concentrate (∼30 μL) and the filtrate (∼470 μL) were transferred to Eppendorf tubes on ice, and their volumes were adjusted to 500 μL with buffer. Then, a few crystals of dithionite were added to each sample followed by BIPY (final concentration of 2 mM), and the concentration of Fe-$[BIPY]_3^{2+}$ (ϵ_{520} = 9000 M^{-1} cm^{-1}) was determined after incubation for 5 min at room temperature in a Beckman DU640B spectrophotometer (*26*). After removal of the retentate, insoluble iron was stripped from the filter by adding 500 μL of buffer containing a few crystals of dithionite and 2 mM BIPY, and by pipetting vigorously for 1 min, followed

by absorbance measurements at 520 nm as described above. Under these conditions, insoluble ferric iron oxides accumulated in the filter of the ultrafiltration device, and the retentate could be removed by pipetting without disturbing the precipitated iron. This was verified by running buffer and apoferritin controls, in the presence of which most iron was reproducibly recovered from the filter and the concentrate, respectively (see the Results). In samples with extensive iron precipitation (buffer at 10 or 60 min, monomeric frataxin or mock at 60 min), the total iron recovery was only 70−80% due to incomplete solubilization of ferric iron oxides from the filter. The iron recovery was ≥90% in all other samples.

RESULTS

Monomeric and Assembled Forms of Human Frataxin Enhance the Availability of Fe(II). Recent reports have described the ability of both yeast and human frataxin to donate iron to IscU, ferrochelatase, and aconitase via intermolecular interactions (*9*, *10*, *16*, *17*), but monomeric and assembled forms of the protein have never been directly compared. We analyzed assembled m-fxn and the m-fxn monomer for their ability to make Fe(II) bioavailable in the presence of atmospheric O_2 at neutral pH, conditions that promote conversion of Fe(II) into insoluble ferric iron oxides. We tested an Fe(II)/subunit ratio of 10/1, close to the iron loading capacity of recombinant human frataxin (*7*, *9*). BIPY, a chelator that preferentially binds Fe(II) (*26*), or purified mouse ferrochelatase, which catalyzes the insertion of Fe(II) into protoporphyrin IX to yield heme (*24*), was used as the Fe(II) ligand. Horse spleen apoferritin, a preassembled 24-subunit shell that promotes iron oxidation and mineralization (*27*), and bovine brain calmodulin, a calcium-binding protein with a molecular mass and an isoelectric point similar to those of m-fxn, were used as controls. Assembled m-fxn kept ferrous iron available to BIPY or ferrochelatase as efficiently as the m-fxn monomer, and over a time course of 60 min, both proteins enhanced Fe(II) availability compared to buffer and controls (Figure 1). However, when the Fe(II)/subunit ratio was decreased from 10/1 to 5/1, the levels of BIPY-accessible Fe(II) decreased by ∼25% in the presence of assembled m-fxn but remained unchanged in the presence of the m-fxn monomer (data not shown). Results similar to those obtained with m-fxn monomer were also obtained with d-fxn monomer (residues 78−210) (not shown), which is the major degradation product of m-fxn both in *E. coli* (*7*) (Figure S1A of the Supporting Information) and in mitochondria (*7*, *23*). This product lacks a nonconserved positively charged amino-terminal region, and was shown by other investigators to serve as an Fe(II) donor *in vitro* (*9*, *10*).

Assembled Frataxin Limits Oxidative Damage to DNA. Next, we examined whether assembled and monomeric m-fxn influence iron-catalyzed DNA strand breakage (*25*). Upon exposure to Fe(II) in buffer, single-strand breaks converted supercoiled DNA to open circular DNA as expected (Figure 2A, lane 2 vs lane 3). In the presence of 20−200 μM assembled m-fxn, supercoiled DNA was also converted to the open circular form upon addition of Fe(II); however, compared to those of the control without protein present, the levels of residual supercoiled DNA increased at increasing concentrations of assembled m-fxn (Figure 2A).

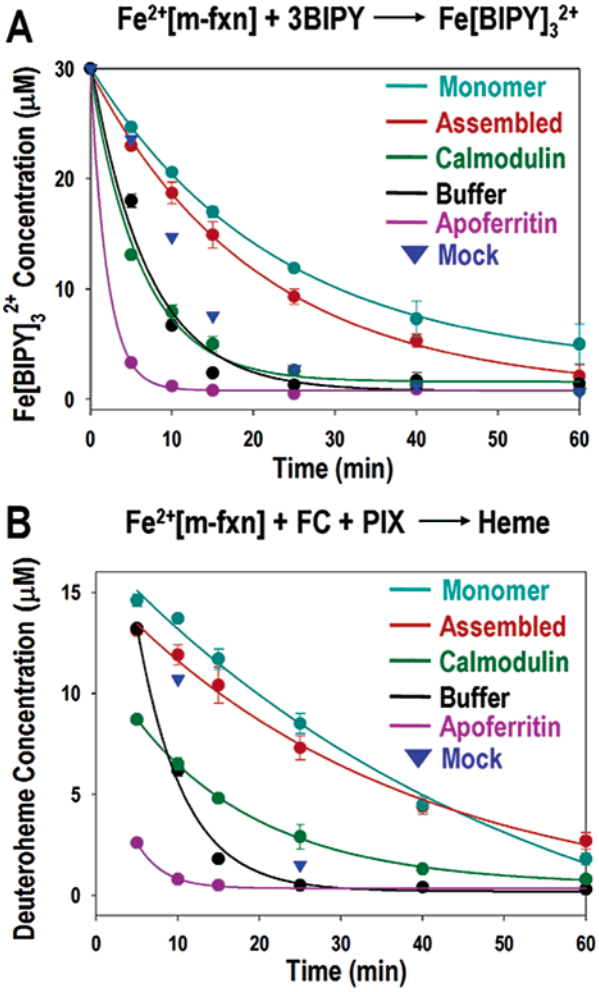

FIGURE 1: Monomeric and assembled forms of human frataxin enhance Fe(II) availability. Time courses of (A) $Fe[BIPY]_3^{2+}$ or (B) deuteroheme production were started by addition of 30 μM Fe(II) to 10 mM HEPES-KOH at pH 7.3 and 30 °C in the absence or presence of 3 μM protein, as indicated. A concentration of contaminating proteins that would be present in 6 μM assembled m-fxn was also tested (mock). At successive time points, aliquots were withdrawn from these reaction mixtures and incubated either with BIPY (2 mM) for 5 min or with ferrochelatase (FC) and deuteroporphyrin IX (PIX) (2 and 120 μM, respectively) for 20 min. The concentrations of the final products, $Fe[BIPY]_3^{2+}$ and deuteroheme (heme), were determined spectrophotometrically (*16*). The bars represent the mean ± the standard deviation of three independent reactions; for mock, $n = 1$.

The levels of residual supercoiled DNA were measured relative to those in reaction mixtures with the same concentrations of assembled m-fxn but no added Fe(II) (Figure 2A, lanes 5, 7, 9, and 11 vs lanes 4, 6, 8, and 10, respectively). This is an accurate measure of protection (*25*), while the level of accumulation of open circular and linear DNA is not a precise measure of damage because these forms can degrade further and their fluorescence in ethidium bromide-stained gels is ∼1.4 times higher than that of supercoiled DNA (*28*). In three independent experiments with assembled m-fxn from different purifications, we determined the following levels of protection (mean ± standard deviation): 58 ± 6, 70 ± 8, 80 ± 5, and 89 ± 6% at Fe(II)/subunit ratios of 10/1, 5/1, 2/1, and 1/1, respectively, as compared to 35 ± 5% in buffer without protein. Preparations of assembled m-fxn contained low levels of background proteins that we were unable to separate (Figure S1A,B of the

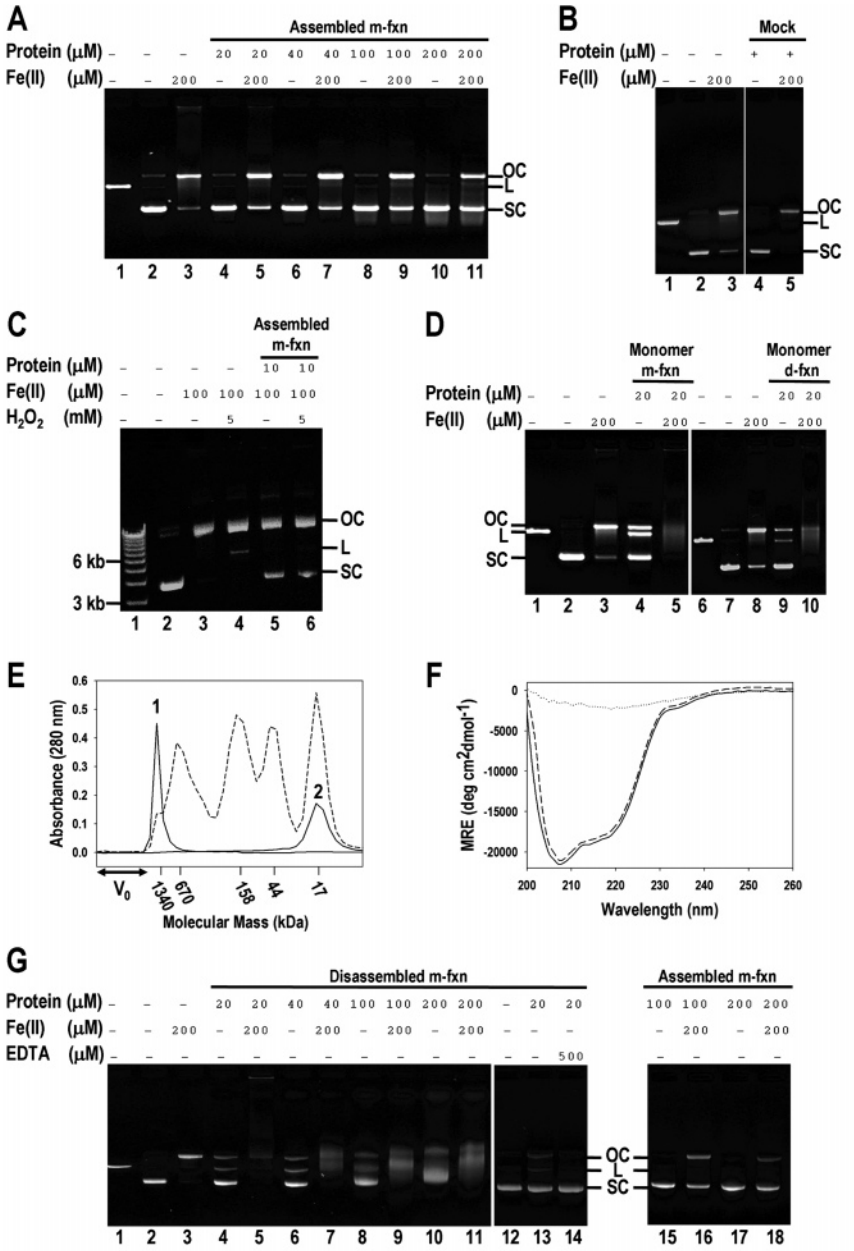

FIGURE 2: Assembled frataxin protects DNA from iron-induced oxidative damage. (A, B, and D) Plasmid DNA was incubated with buffer, different concentrations of purified forms of frataxin, or a concentration of contaminating proteins that would be present in 200 μM assembled m-fxn (mock; Figure S1C of the Supporting Information). Reactions were started by addition of ferrous iron or an equivalent volume of buffer. At the end of 20 min at 30 °C, the sample buffer was added and the samples were immediately analyzed by agarose gel electrophoresis. Lane 1 contained the *Xho*I digest of plasmid DNA (~3000 bp). SC, OC, and L represent supercoiled, open circular, and linear DNA, respectively. (C) Plasmid DNA (~6000 bp) was incubated with buffer or assembled m-fxn as shown. Reactions were started by addition of hydrogen peroxide immediately followed by ferrous iron. Samples were incubated at 30 °C for 10 min and analyzed as described above. Lane 1 contained MW marker. (E) Sephacryl 300 chromatograms of buffer-treated (peak 1) or SDS-treated (peak 2) assembled m-fxn. Molecular masses (- - -) and V_0 were determined with Bio-Rad protein standards and formalin-fixed *Streptomyces aureus*. (F) CD spectra were recorded between 260 and 200 nm. The monomer from *E. coli* (- - -) or from SDS-treated assembled m-fxn (—) (7 μM each) was scanned at 5 °C; the thermally denatured monomer (7 μM) from *E. coli* was scanned at 90 °C (•••). Measurements were taken every 1 nm with an averaging time of 25 s/measurement. (G) Experimental conditions were as described for panels A and B, except that plasmid DNA was incubated in buffer, or with different concentrations of SDS-treated (disassembled) or buffer-treated (assembled) m-fxn, each repurified by gel filtration as shown in panel D. Lane 1 contained the *Xho*I digest of plasmid DNA; lane 14 contained plasmid DNA preincubated with 500 μM EDTA for 10 min on ice.

Supporting Information). Mock protein preparations from *E. coli* transformed with the empty vector contained comparable levels of the same background proteins (Figure S1C of the Supporting Information) but had no protective effect relative to buffer (Figure 2B, lane 5 vs lane 3), indicating that this is a specific property of assembled m-fxn. Assembled m-fxn protected DNA even upon addition of Fe(II) and hydrogen peroxide (Figure 2C, lane 6 vs lane 4), implying that it can attenuate Fenton chemistry, similar to certain bacterial ferritins (*29*, *30*). In contrast, DNA was converted to both the open circular and linear forms in the presence of 20 μM m-fxn monomer or d-fxn monomer, and this damage was dramatically enhanced upon addition of Fe(II) (Figure 2D, lanes 4, 5, 9, and 10). Because the purified assembled m-fxn

did not damage DNA in the absence of exogenous Fe(II) (Figure 2A, lanes 4, 6, 8, and 10 vs lane 2), we used it as an alternative source of the monomer. A preparation of assembled m-fxn was divided in two halves that were incubated with 2% SDS or buffer, treated identically with a detergent removal resin, and further purified through a new gel filtration column. The buffer-treated frataxin eluted with an apparent molecular mass of >1 MDa as expected, and the SDS-treated frataxin with an apparent molecular mass of 17 kDa corresponding to the m-fxn monomer (Figure 2E). As determined by far-UV CD, SDS-treated m-fxn exhibited the same fold and melting temperature as the monomer purified from *E. coli* (Figure 2F and data not shown). These data indicate that even if trace amounts of SDS were still bound to the disassembled monomer, they did not affect its structure to a significant degree. In the presence of disassembled m-fxn, supercoiled DNA was once again converted to both the open circular and linear forms in a protein concentration-dependent manner (Figure 2G, lanes 4, 6, 8, and 10). This damage was inhibited when DNA was preincubated with EDTA (lanes 13 and 14), but was enhanced upon addition of Fe(II) (lanes 5, 7, 9, and 11). In contrast, the buffer-treated assembled frataxin did not cause DNA damage (Figure 2G, lanes 15 and 17 vs lane 2), and attenuated it upon addition of Fe(II) in an Fe(II)/subunit ratio-dependent manner (lanes 16 and 18 vs lane 3), confirming the results depicted in Figure 2A.

Assembled Frataxin Sequesters Redox-Active Iron from the Solution. The data presented above suggest that monomeric and assembled m-fxn have different modes of handling redox-active iron. We investigated this possibility under the conditions used in Figure 1, where the m-fxn monomer and assembled m-fxn were able to keep similar levels of Fe(II) accessible to BIPY or ferrochelatase over a period of 60 min. Proteins were incubated with Fe(II) for 10 or 60 min, and after ultrafiltration, iron levels were measured in the retentate [representing the sum of free and protein-bound Fe(II)], the filtrate [representing free Fe(II) removed from the reaction mixture during ultrafiltration], and the insoluble fraction [representing Fe(III) that undergoes spontaneous hydrolysis and precipitates out of the solution]. In buffer without protein, we recovered mostly insoluble Fe(III) at either 10 or 60 min, while in the presence of apoferritin, most iron was in the retentate (Figure 3). In the presence of monomeric frataxin (m-fxn or d-fxn monomer), free Fe(II) was predominant at 10 min but mostly insoluble Fe(III) was recovered at 60 min (Figure 3). The same was observed with mock preparations of assembled m-fxn (Figure 3). Assembled m-fxn exhibited equal levels of iron in the retentate, filtrate, and insoluble fraction at 10 min, but a striking difference was seen at 60 min when most iron was recovered in the retentate (Figure 3). These results can be interpreted as follows. In the reaction mixture, free Fe(II) is in an equilibrium with protein-bound Fe(II):

$$\text{Fe(II)} + \text{protein} \leftrightarrow \text{Fe(II)}-\text{protein}$$

In the presence of the monomer, free Fe(II) is progressively removed from the reaction mixture by conversion to insoluble ferric oxides, and the equilibrium is maintained via release of Fe(II) from the protein until most Fe(II) is converted to ferric oxides, as seen in Figure 3 at 60 min. At 10 min, iron

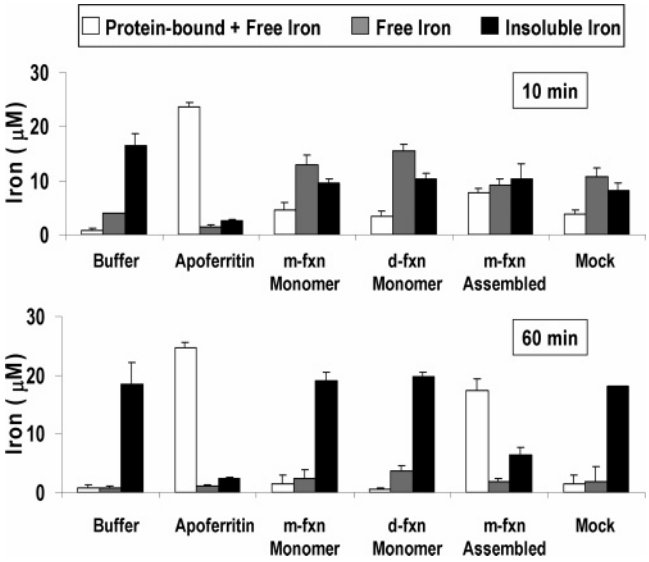

FIGURE 3: Assembled but not monomeric frataxin stores Fe(III) in soluble form. Purified proteins (3 μM) or a concentration of contaminating proteins that would be present in 6 μM assembled m-fxn (mock) was incubated with 30 μM Fe(II) for 10 or 60 min in 10 mM HEPES-KOH at pH 7.3 and 30 °C, and subjected to ultrafiltration. Iron levels were measured in the retentate, the filtrate, and the insoluble fraction by addition of dithionite followed by BIPY (*16*) as described in Materials and Methods. Bars represent the mean ± the standard deviation from three (apoferritin, buffer, and d-fxn monomer), five (assembled m-fxn), seven (m-fxn monomer), or two (mock) independent experiments. A paired *t* test comparing protein-bound, filterable, and insoluble iron for each frataxin from 10 min vs 60 min yielded *P* values of <0.05 in all cases.

levels in the filtrate are higher than in the retentate because the removal of free Fe(II) from the reaction mixture during ultrafiltration results in further release of Fe(II) from the monomer. In the presence of assembled m-fxn, the Fe(II)−protein is removed from the reaction mixture via conversion to a stable Fe(III)−protein complex, faster than free Fe(II) is converted to insoluble ferric oxides. Here, the equilibrium is shifted toward binding of Fe(II) to protein until most Fe(II) is converted to stable Fe(III)−protein complexes, as seen from the data at 10 and 60 min. In this way, assembled frataxin achieves nearly the same degree of iron uptake as apoferritin, only with slower kinetics (Figure 3).

Assembled Human Frataxin Has Ferroxidase Activity. We used electrode oximetry to examine the iron oxidation reaction of monomeric and assembled m-fxn. Solution conditions were chosen on the basis of our previous analysis of the ferroxidase activity of yeast frataxin (*34*). To observe this activity, the pH must be ≤7.0 to inhibit iron autoxidation, and the Fe(II) concentration must not exceed the number of ferroxidation sites on the protein. Similar conditions are required to observe the ferroxidase activity of H-ferritin (*35*). Oxygen consumption curves were recorded upon addition of Fe(II) to buffer alone or buffer containing assembled m-fxn, the m-fxn monomer, or the mock preparation. In Figure 4A, we compare the Fe(II)/O_2 stoichiometries for the completed reactions of monomeric and assembled m-fxn at increasing Fe(II)/subunit ratios. A final stoichiometric ratio of ∼2 Fe(II) atoms oxidized per O_2 molecule consumed was consistently measured in the presence of assembled m-fxn at Fe(II)/subunit ratios of ≤0.75, while the Fe(II)/O_2 stoichiometry approached a value of ∼4 at higher ratios (Figure

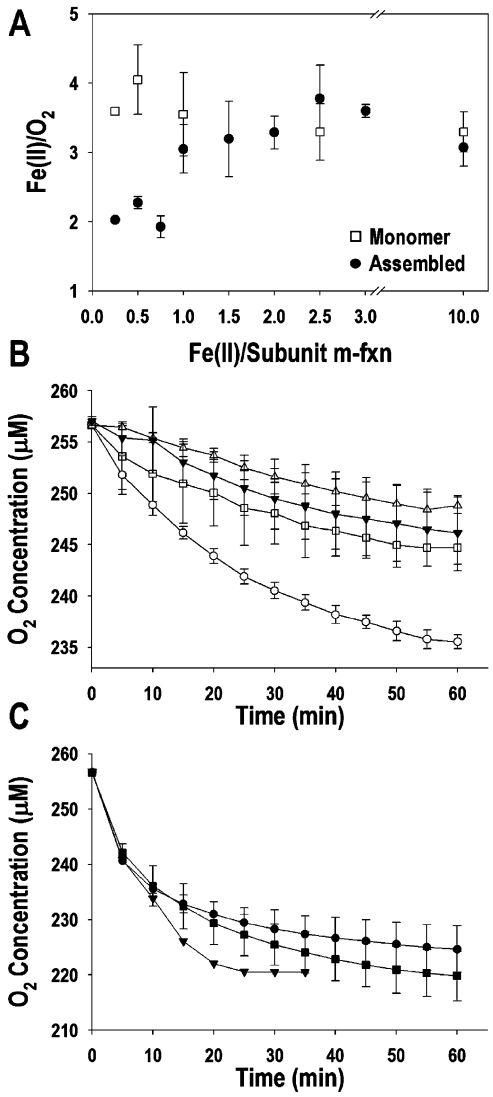

FIGURE 4: Assembled frataxin has ferroxidase activity. (A) The stoichiometric Fe(II)/O_2 ratios measured in the presence of monomeric or assembled m-fxn are plotted vs the Fe(II)/m-fxn subunit ratio. Oxygen consumption was monitored upon addition of Fe(II) to buffer in the presence of the m-fxn monomer or assembled m-fxn at increasing Fe(II)/subunit ratios. Conditions were 10 mM HEPES-KOH at pH 7.0 and 25 °C at Fe(II)/subunit ratios between 0.25/1 and 3/1 or 10 mM HEPES-KOH at pH 7.3 and 30 °C at the Fe(II)/subunit ratio of 10/1 (at this ratio, autoxidation predominates regardless of the solution conditions). The Fe(II)/O_2 ratio was measured at the end of each reaction (~60 and 40 min in the first and second set of solution conditions, respectively). Some reactions were followed for as long as 120 min without any significant changes in the final Fe(II)/O_2 stoichiometry (not shown). Each point represents the mean ± the standard deviation from two to three reactions, except at an Fe(II)/subunit ratio of 0.25 where $n = 1$. The protein concentration was 96 μM at Fe(II)/subunit ratios of 0.25/1 and 0.5/1, 48 μM at Fe(II)/subunit ratios between 0.75/1 and 3.0/1, and 10 μM at an Fe(II)/subunit ratio of 10/1. Buffer controls without protein added were carried out under the same conditions used for monomeric and assembled m-fxn, and gave a mean stoichiometric Fe(II)/O_2 ratio of 3.6 ± 0.4 ($n = 29$) in 10 mM HEPES-KOH at pH 7.0, 25 °C, and 3.5 ± 0.06 ($n = 3$) in 10 mM HEPES-KOH at pH 7.3 and 30 °C. (B and C) Oxygen consumption was monitored upon addition of (B) 48 μM Fe(II) to buffer (▼) in the absence or presence of the mock preparation (△), 96 μM monomer (□), or 96 μM assembled m-fxn (○) [Fe(II)/subunit ratio of 0.5/1] or (C) 120 μM Fe(II) to buffer (▼), 48 μM monomer (■), or 48 μM assembled m-fxn (●) [Fe(II)/subunit ratio of 2.5/1]. In panels B and C, conditions were 10 mM HEPES-KOH at pH 7.0 and 25 °C. Mock controls contained a concentration of contaminating proteins that would be present in 200 μM assembled m-fxn. Bars represent the standard deviation of two or three (monomer, assembled, and mock) or six (buffer) independent reactions; one representative buffer run is shown in panel C.

4A). These results are consistent with predominant ferroxidase activity when ≤0.75 equiv of Fe(II) is added to assembled m-fxn, with autoxidation overriding ferroxidation at higher Fe(II)/subunit ratios (*35*). In contrast, the average Fe(II)/O_2 stoichiometry for the completed reactions of the m-fxn monomer was ~3.6 (Figure 4A), indicating that autoxidation is the predominant reaction that occurs with this form of the protein regardless of the Fe(II)/subunit ratio. Figure 4B shows facilitation of iron oxidation in the presence of assembled m-fxn compared to the buffer, monomer, or mock at an Fe(II)/subunit ratio of 0.5. Facilitation of iron oxidation by assembled m-fxn was also observed at Fe(II)/subunit ratios of 0.25 and 0.75 as well as at an Fe(II)/subunit ratio of 0.5 in the presence of 150 mM KCl, even though chloride anions significantly decreased the rate of spontaneous iron oxidation (not shown). However, at Fe(II)/subunit ratios of >0.75, the iron oxidation reactions of the m-fxn monomer and assembled m-fxn occurred at similar rates and took twice as long as the reaction in buffer without protein to reach completion (Figure 4C and data not shown). The ability of yeast and *E. coli* frataxin to facilitate pairwise oxidation of Fe(II) has led to suggestions that dinuclear iron binding sites may be present on these proteins (*11*, *34*). In vertebrate ferritins, there is one dinuclear iron site on each H-subunit, and to observe ferroxidase activity, the iron concentration must be ≤2 Fe(II) atoms/H-subunit to not exceed the number of ferroxidation sites (*35*). Figure 4A shows that to observe the ferroxidase activity of assembled m-fxn, the iron concentration must be <1 Fe(II) atom/subunit, consistent with the presence of less than one ferroxidation site per subunit, as was suggested previously for yeast frataxin (*34*). A ferroxidation site formed by multiple m-fxn subunits supports the conclusion that assembly is required for the ferroxidase activity of human frataxin.

DISCUSSION

Mitochondrial function depends on a continuous supply of iron for the syntheses of heme and ISC, but also on the prevention of iron toxicity, especially iron-induced oxidative damage to mitochondrial DNA. Accumulated evidence indicates that the mitochondrial protein frataxin plays a key role in both of these processes (*5*). To begin to understand how frataxin may accomplish both iron chaperone and iron detoxification functions, we have analyzed stable monomeric and assembled forms of human frataxin. Both forms bind ~6−10 Fe atoms/protomer (*7*, *9*) and promote the availability of Fe(II) (Figure 1). The conditions used in these experiments are different from the situation in the mitochondrial matrix, where a number of factors (e.g., a pH of ~8 and the presence of physiologic iron chelators and reducing agents) may influence Fe(II) availability. On the other hand, other investigators have shown that mitochondria of frataxin-deficient yeast cells accumulate iron in amorphous nanoparticles of ferric phosphate, which is unavailable for heme synthesis (*15*). These findings suggest that the ability of monomeric and assembled frataxin to make Fe(II) available to ferrochelatase *in vitro* is a physiologically relevant property.

Unlike monomeric frataxin, the assembled form exhibits additional properties, including ferroxidase activity, the ability to sequester Fe(II) from bulk solution and to store it

in a water soluble form as well as the ability to limit iron-catalyzed oxidative damage to DNA (Figures 2−4). As determined by electrospray ionization mass spectrometry, the molecular mass of the monomer obtained from acetonitrile-denatured assembled m-fxn is the same, within error, as that of the monomer purified from *E. coli* (17 755 Da vs 17 752 Da). This should rule out the possibility that the functional differences observed between assembled and monomeric m-fxn result from there being two different types of monomers due to post-translational modifications. In addition, disassembled m-fxn and the monomer purified from *E. coli* were both unable to protect DNA to an equivalent degree (Figure 2D−G), supporting the conclusion that the association state of the protein is responsible for the DNA protection conferred by assembled m-fxn (Figure 2A,G). Moreover, the results depicted in Figure 4A are consistent with a ferroxidation site formed by more than one m-fxn subunit, supporting the conclusion that m-fxn self-assembly is responsible for ferroxidase activity. Recent studies investigating the mechanism of m-fxn assembly have revealed that this process involves stable subunit−subunit interactions mediated by the N-terminal domain of m-fxn and a reversible conformational change (*37*). Because m-fxn assembles in *E. coli* and mitochondria but not *in vitro* (*7*, *37*), molecular chaperones and other factors are probably also required. A lack of these factors may explain why the purified m-fxn monomer does not self-associate.

The protective effect of assembled m-fxn appears to result from the ability to sequester Fe(II) from the solution and to promote the formation of a stable mineral within a protein-protected compartment (Figure 3). In agreement with this interpretation, previous studies have shown that assembled human frataxin accumulates iron as small ∼2−4 nm electron-dense cores that appear to be situated within the boundaries of the protein particles (*7*). In addition, an X-ray spectroscopic study of yeast and human frataxin iron cores showed that they consist of a ferric oxide mineral structurally similar to ferrihydrite (*31*). The three-dimensional structures of the human frataxin monomer have revealed an extended anionic surface formed by the side chains of aspartic and glutamic acid residues (*32*, *33*). No structural information is as yet available for assembled frataxin, but we speculate that this form of the protein may contain a cavity lined by the anionic surfaces of adjacent subunits, similar to the inner cavity involved in the iron uptake mechanism of the ferritins (*27*). The ferritins are polymers of 12 or 24 subunits that form a protein shell with a hollow cavity accommodating up to 4500 atoms of iron. Ferritin binds Fe(II), catalyzes its oxidation to Fe(III), and further incorporates Fe(III) into a water-soluble mineral core (*27*). The molecular design of ferritin is conserved across species, underscoring the advantage of using protein assembly to detoxify and store iron within the cell. Therefore, it is plausible that assembly may also be a mechanism utilized by frataxin to detoxify iron within mitochondria. This hypothesis is in line with the oxidative damage associated with a loss or reduction of frataxin (*20*, *21*), and is supported by a recent report that the expression of human mitochondrial ferritin results in nearly full complementation of frataxin-deficient yeast (*22*). However, the ferroxidase reaction of assembled m-fxn is much slower than that of mammalian ferritin (minutes vs seconds; Figure 4B, data not shown, and ref *36*), and is readily overcome by an

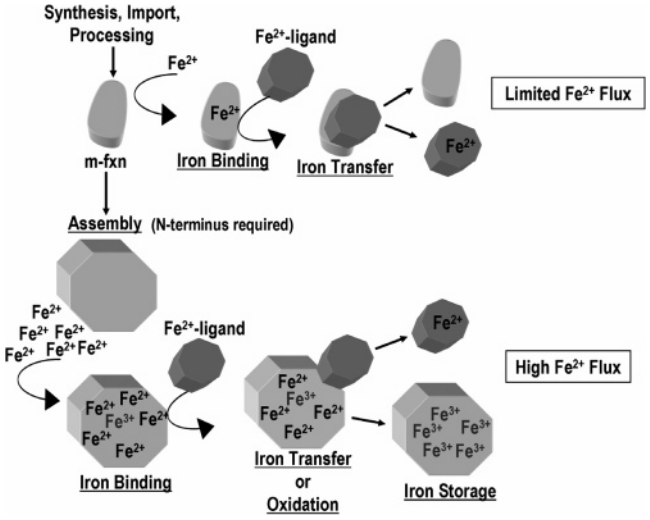

FIGURE 5: Proposed mechanism of human frataxin. A putative Fe(II) ligand (e.g., IscU) is shown as a soluble molecule with one Fe(II)-binding site. The human frataxin monomer may act as a donor of Fe(II) when mitochondrial iron is limited. Given the observed inability of the monomer to control the solution chemistry of iron, any Fe(II) bound to it is rapidly and quantitatively transferred to a ligand to prevent oxidative damage. In the presence of a high iron flux, assembled frataxin sequesters Fe(II), makes it bioavailable, and further detoxifies any excess iron by promoting its oxidation and incorporation into a stable mineral (*31*).

even slower autoxidation reaction at Fe(II)/subunit ratios of >0.75 (Figure 4C and data not shown). Iron autoxidation occurs at similar rates in the presence of assembled and monomeric m-fxn, and is slower compared to iron autoxidation in buffer (Figure 4C and data not shown). These features enable assembled and monomeric frataxin to serve as temporary reservoirs of readily available Fe(II) (Figure 1). It is intriguing that both monomeric and assembled m-fxn can make Fe(II) available to external ligands, yet the two forms have such different effects on protection against Fe-induced DNA damage. At a fixed iron concentration in the presence of assembled m-fxn, the levels of BIPY-accessible Fe(II) decrease at increasing Fe(II)/subunit ratios (data not shown). This suggests that the Fe(II)/subunit ratio is an important factor in determining the extent to which the Fe(II) bound to assembled frataxin is accessible to external ligands. It seems logical that this Fe(II) should also be available for free radical generation, and indeed, the ability to protect DNA decreased from 89 to 58% when the Fe(II)/subunit ratio was increased from 1/1 to 10/1 (Results and Figure 2A). However, in these *in vitro* assays, we could only analyze the Fe(II) chaperone and antioxidant functions of assembled frataxin independent of each other. It is conceivable that *in vivo* the protein might carry out these two functions simultaneously, promoting incorporation of Fe(II) into heme or iron−sulfur clusters and oxidizing and storing any surplus iron such that little or no Fe(II)-bound frataxin would be available for free radical generation. Thus, we speculate that monomeric and assembled forms of human frataxin serve different physiological roles depending on the magnitude of the mitochondrial iron flux (Figure 5). The factors that govern assembly of human frataxin may provide mitochondria with a mechanism for promoting iron metabolism and for limiting iron-induced oxidative damage.

ACKNOWLEDGMENT

We are indebted to our colleagues, Drs. L. James Maher III, Marina Ramirez-Alvarado, Piero Rinaldo, and Natalia Khaylova, at the Mayo Clinic College of Medicine, for their expert assistance and valuable advice.

SUPPORTING INFORMATION AVAILABLE

Modifications to the m-fxn purification procedure, a figure showing SDS−PAGE analysis of the m-fxn monomer, assembled m-fxn, and mock preparations, and a list of the contaminating proteins identified in assembled m-fxn preparations. This material is available free of charge via the Internet at http://pubs.acs.org.

REFERENCES

1. Campuzano, V., Montermini, L., Molto, M. D., Pianese, L., Cossee, M., Cavalcanti, F., Monros, E., Rodius, F., Duclos, F., Monticelli, A., et al. (1996) Friedreich's ataxia: Autosomal recessive disease caused by an intronic GAA triplet repeat expansion, *Science 271*, 1423−1427.
2. Babcock, M., de Silva, D., Oaks, R., Davis-Kaplan, S., Jiralerspong, S., Montermini, L., Pandolfo, M., and Kaplan, J. (1997) Regulation of mitochondrial iron accumulation by Yfh1p, a putative homolog of frataxin, *Science 276*, 1709−1712.
3. Foury, F., and Cazzalini, O. (1997) Deletion of the yeast homologue of the human gene associated with Friedreich's ataxia elicits iron accumulation in mitochondria, *FEBS Lett. 411*, 373−377.
4. Wilson, R. B., and Roof, D. M. (1997) Respiratory deficiency due to loss of mitochondrial DNA in yeast lacking the frataxin homologue, *Nat. Genet. 16*, 352−357.
5. Pandolfo, M. (2003) Friedreich ataxia, *Semin. Pediatr. Neurol. 10*, 163−172.
6. Adamec, J., Rusnak, F., Owen, W. G., Naylor, S., Benson, L. M., Gacy, A. M., and Isaya, G. (2000) Iron-Dependent Self-Assembly of Recombinant Yeast Frataxin: Implications for Friedreich Ataxia, *Am. J. Hum. Genet. 67*, 549−562.
7. Cavadini, P., O'Neill, H. A., Benada, O., and Isaya, G. (2002) Assembly and iron binding properties of human frataxin, the protein deficient in Friedreich ataxia, *Hum. Mol. Genet. 33*, 217−227.
8. Adinolfi, S., Trifuoggi, M., Politou, A. S., Martin, S., and Pastore, A. (2002) A structural approach to understanding the iron-binding properties of phylogenetically different frataxins, *Hum. Mol. Genet. 11*, 1865−1877.
9. Yoon, T., and Cowan, J. A. (2003) Iron−sulfur cluster biosynthesis. Characterization of frataxin as an iron donor for assembly of [2Fe-2S] clusters in ISU-type proteins, *J. Am. Chem. Soc. 125*, 6078−6084.
10. Yoon, T., and Cowan, J. A. (2004) Frataxin-mediated iron delivery to ferrochelatase in the final step of heme biosynthesis, *J. Biol. Chem. 279*, 25943−25946.
11. Bou-Abdallah, F., Adinolfi, S., Pastore, A., Laue, T. M., and Chasteen, N. D. (2004) Iron binding and oxidation kinetics in frataxin CyaY of *Escherichia coli*, *J. Mol. Biol. 341*, 605−615.
12. Muhlenhoff, U., Richhardt, N., Ristow, M., Kispal, G., and Lill, R. (2002) The yeast frataxin homolog Yfh1p plays a specific role in the maturation of cellular Fe/S proteins, *Hum. Mol. Genet. 11*, 2025−2036.
13. Duby, G., Foury, F., Ramazzotti, A., Herrmann, J., and Lutz, T. (2002) A non-essential function for yeast frataxin in iron−sulfur cluster assembly, *Hum. Mol. Genet. 11*, 2635−2643.
14. Seznec, H., Simon, D., Monassier, L., Criqui-Filipe, P., Gansmuller, A., Rustin, P., Koenig, M., and Puccio, H. (2004) Idebenone delays the onset of cardiac functional alteration without correction of Fe−S enzymes deficit in a mouse model for Friedreich ataxia, *Hum. Mol. Genet. 13*, 1017−1024.
15. Lesuisse, E., Santos, R., Matzanke, B. F., Knight, A. A. B., Camadro, J. M., and Dancis, A. (2003) Iron use for heme synthesis is under control of the yeast frataxin homologue (Yfh1), *Hum. Mol. Genet. 12*, 879−889.
16. Park, S., Gakh, O., O'Neill, H. A., Mangravita, A., Nichol, H., Ferreira, G. C., and Isaya, G. (2003) Yeast frataxin sequentially chaperones and stores iron by coupling protein assembly with iron oxidation, *J. Biol. Chem. 278*, 31340−31351.
17. Bulteau, A. L., O'Neill, H. A., Kennedy, M. C., Ikeda-Saito, M., Isaya, G., and Szweda, L. I. (2004) A novel role of frataxin as an iron chaperone protein required for pro-oxidant induced modulation of mitochondrial aconitase activity, *Science 305*, 242−245.
18. Tan, G., Chen, L. S., Lonnerdal, B., Gellera, C., Taroni, F. A., and Cortopassi, G. A. (2001) Frataxin expression rescues mitochondrial dysfunctions in FRDA cells, *Hum. Mol. Genet. 10*, 2099−2107.
19. Wong, A., Yang, J., Cavadini, P., Gellera, C., Lonnerdal, B., Taroni, F., and Cortopassi, G. (1999) The Friedreich's ataxia mutation confers cellular sensitivity to oxidant stress which is rescued by chelators of iron and calcium and inhibitors of apoptosis, *Hum. Mol. Genet. 8*, 425−430.
20. Bradley, J. L., Homayoun, S., Hart, P. E., Schapira, A. H., and Cooper, J. M. (2004) Role of oxidative damage in Friedreich's ataxia, *Neurochem. Res. 29*, 561−567.
21. Karthikeyan, G., Santos, J. H., Graziewicz, M. A., Copeland, W. C., Isaya, G., van Houten, B., and Resnick, M. A. (2003) Reduction in frataxin causes progressive accumulation of mitochondrial damage, *Hum. Mol. Genet. 12*, 3331−3342.
22. Campanella, A., Isaya, G., O'Neill, H., Santambrogio, P., Cozzi, A., Arosio, P., and Levi, S. (2004) The expression of human mitochondrial ferritin rescues respiratory function in frataxin-deficient yeast, *Hum. Mol. Genet. 13*, 2279−2288.
23. Cavadini, P., Adamec, J., Taroni, F., Gakh, O., and Isaya, G. (2000) Two-step processing of human frataxin by mitochondrial processing peptidase: Precursor and intermediate forms are cleaved at different rates, *J. Biol. Chem. 275*, 41469−41475.
24. Ferreira, G. C. (1994) Mammalian ferrochelatase. Overexpression in *Escherichia coli* as a soluble protein, purification and characterization, *J. Biol. Chem. 269*, 4396−4400.
25. Toyokuni, S., and Sagripanti, J. L. (1992) Iron-mediated DNA damage: Sensitive detection of DNA strand breakage catalyzed by iron, *J. Inorg. Biochem. 47*, 241−248.
26. Richards, T. D., Pitts, K. R., and Watt, G. D. (1996) A kinetic study of iron release from *Azotobacter vinelandii* bacterial ferritin, *J. Inorg. Biochem. 61*, 1−13.
27. Chasteen, N. D., and Harrison, P. M. (1999) Mineralization in ferritin: An efficient means of iron storage, *J. Struct. Biol. 126*, 182−194.
28. Chaston, T. B., and Richardson, D. R. (2003) Interactions of the pyridine-2-carboxaldehyde isonicotinoyl hydrazone class of chelators with iron and DNA: Implications for toxicity in the treatment of iron overload disease, *J. Biol. Inorg. Chem. 8*, 427−438.
29. Zhao, G., Ceci, P., Ilari, A., Giangiacomo, L., Laue, T. M., Chiancone, E., and Chasteen, N. D. (2002) Iron and hydrogen peroxide detoxification properties of DNA-binding protein from starved cells. A ferritin-like DNA-binding protein of *Escherichia coli*, *J. Biol. Chem. 277*, 27689−27696.
30. Bou-Abdallah, F., Lewin, A. C., Le Brun, N. E., Moore, G. R., and Chasteen, N. D. (2002) Iron detoxification properties of *Escherichia coli* bacterioferritin. Attenuation of oxyradical chemistry, *J. Biol. Chem. 277*, 37064−37069.
31. Nichol, H., Gakh, O., O'Neill, H. A., Pickering, I. J., Isaya, G., and George, G. N. (2003) Structure of frataxin iron cores: An X-ray absorption spectroscopic study, *Biochemistry 42*, 5971−5976.
32. Musco, G., Stier, G., Kolmerer, B., Adinolfi, S., Martin, S., Frenkiel, T., Gibson, T., and Pastore, A. (2000) Towards a structural understanding of Friedreich's ataxia: The solution structure of frataxin, *Struct. Folding Des. 8*, 695−707.
33. Dhe-Paganon, S., Shigeta, R., Chi, Y. I., Ristow, M., and Shoelson, S. E. (2000) Crystal structure of human frataxin, *J. Biol. Chem. 275*, 30753−30756.

34. Park, S., Gakh, O., Mooney, S. M., and Isaya, G. (2002) The ferroxidase activity of yeast frataxin, *J. Biol. Chem. 277*, 38589−38595.
35. Yang, X., and Chasteen, N. D. (1999) Ferroxidase activity of ferritin: Effects of pH, buffer and Fe(II) and Fe(III) concentrations on Fe(II) autoxidation and ferroxidation, *Biochem. J. 338*, 615−618.
36. Yang, X., Chen-Barrett, Y., Arosio, P., and Chasteen, N. D. (1998) Reaction paths of iron oxidation and hydrolysis in horse spleen and recombinant human ferritins, *Biochemistry 37*, 9743−9750.
37. O'Neill, H. A., Gakh, O., and Isaya, G. (2005) Supramolecular assemblies of human frataxin are formed via subunit−subunit interactions mediated by a non-conserved amino-terminal region. *J. Mol. Biol. 345*, 433−439.

BI048459J